

## Microsecond Resolution of Quasiparticle Tunneling in the Single-Cooper-Pair Transistor

A. J. Ferguson,\* N. A. Court, F. E. Hudson, and R. G. Clark

*Australian Research Centre of Excellence for Quantum Computer Technology, University of New South Wales, Sydney NSW 2052, Australia*

(Received 12 April 2006; published 7 September 2006)

We present radio-frequency measurements on a single-Cooper-pair-transistor in which individual quasiparticle poisoning events were observed with microsecond temporal resolution. Thermal activation of the quasiparticle dynamics is investigated, and consequently, we are able to determine energetics of the poisoning and unpoisoning processes. In particular, we are able to assign an effective quasiparticle temperature to parametrize the poisoning rate.

DOI: [10.1103/PhysRevLett.97.106603](https://doi.org/10.1103/PhysRevLett.97.106603)

PACS numbers: 72.20.Jv, 73.23.Hk, 85.25.Cp

Operation of both the single-Cooper-pair transistor (SCPT) and the Cooper-pair-box (CPB) rely on the coherent tunneling of a single Cooper pair between a reservoir and a tunnel-coupled island. This coherent phenomenon is the basis of CPB charge qubits [1,2] and low-dissipation electrometry using the SCPT [3,4]. One of the challenges that faces these devices is avoiding the incoherent tunneling of quasiparticles, often referred to as quasiparticle poisoning. The effect of quasiparticle poisoning is to change the charge on the device island by an electron and halt the coherent tunneling of Cooper pairs. This is especially undesirable for the CPB qubit where it can be a major source of decoherence [5,6].

Quasiparticle poisoning has been extensively studied with a wide variation in behavior observed [4,7–10]. However, a model suggested by Aumentado *et al.* appears to successfully explain the phenomenon [11]. In this model there is some unknown (and possibly nonequilibrium) source of quasiparticles in the device leads. These quasiparticles are able to tunnel onto (poisoning) the device island which usually acts as a quasiparticle trap. Subsequently the trapped quasiparticle is thermally excited (unpoisoning) out of the trap, and the island returns to its even state.

While most previous investigations of quasiparticle poisoning have been performed with a relatively low bandwidth, we note a very recent careful study of oxygen-doped aluminum SCPTs measured by an rf technique sensitive to the Josephson inductance [12]. In that case, detailed measurements of the temperature dependence of the poisoned-state lifetime allowed determination of a quasiparticle trap depth on the island. In this Letter we present measurements of a SCPT, made by a different technique, embedded in a related radio-frequency (rf) tank circuit. A temperature dependent study allowed the energetics of both the poisoning and unpoisoning processes to be determined. In particular, a measurement of the thermal activation of the unpoisoned-state lifetime enabled an effective quasiparticle temperature to be deduced which is an experimentally useful way to parametrize quasiparticle poisoning.

We engineer the SCPT to have a greater superconducting gap ( $2\Delta$ ) for the island than the leads  $\Delta_i > \Delta_l$  [11] by making use of the rapid enhancement of  $\Delta$  with decreasing film thickness [13,14] [Fig. 1(c)]. This reduces the depth of the quasiparticle trap, allowing quasiparticles to be more easily thermally excited out from the island. The island is made from a 10 nm thick film ( $\Delta_i = 250 \pm 15 \mu\text{eV}$ ) while the leads have a thickness of 30 nm ( $\Delta_l = 208 \pm 10 \mu\text{eV}$ ), with  $\Delta$  determined by measuring the onset of quasiparticle tunneling in semiconductor-insulator-semiconductor (SIS) junctions. The device pattern [Fig. 1(a)] is defined in polymer bilayer resist by electron beam lithography and the aluminum thermally evaporated at a rate of  $0.1 \text{ nm s}^{-1}$  onto a liquid-nitrogen-cooled stage. With this technique we were able to achieve electrically continuous films down to a thickness of 5 nm [15]. A controlled oxidization (35 mTorr for 2 minutes) between the evaporations defines the tunnel barriers.

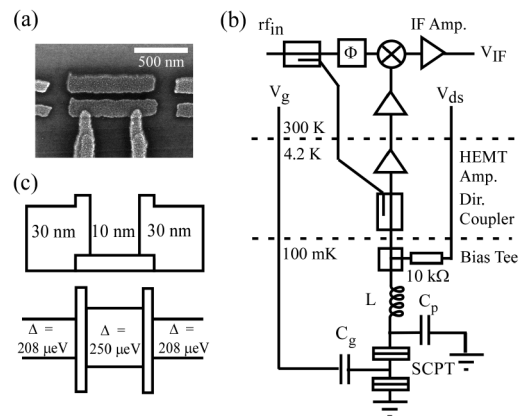


FIG. 1. (a) Scanning electron micrograph of the device. (b) Simplified rf circuit diagram. The rf-carrier signal reflected from the tank circuit is amplified by a cryogenic amplifier with a gain of 38 dB at 4.2 K. After a further 30 dB of amplification at room temperature, the carrier is phase shifted and homodyne detected. (c) Profile of the SCPT showing aluminum film thickness and the resulting change in  $\Delta$ .

The circuit used for this experiment is the same as commonly used for the radio-frequency single-electron transistor (rf-SET) [Fig. 1(b)] [16,17]. A resonant circuit at 326 MHz is formed by a chip inductor ( $L = 470$  nH), a parasitic capacitance ( $C_p = 0.51$  pF), and the SCPT. The reflection coefficient ( $S_{11} = |Z_T - 50/Z_T + 50|$ ) of a small ( $\sim 1$   $\mu$ V) incident rf-carrier signal at the circuit resonance ( $\omega^2 = 1/LC$ ) is determined by mismatch of the tank circuit impedance ( $Z_T = L/RC$ ) to a 50  $\Omega$  coaxial cable. The reflected carrier signal is then amplified by a low-noise cryogenic amplifier. Following further amplification at room temperature, the rf carrier is demodulated by mixing with a local oscillator at the carrier frequency (a technique sensitive to both phase and amplitude of the reflected rf carrier). The resulting intermediate frequency (IF) output is further amplified and recorded on an oscilloscope.

When Coulomb diamonds are measured a  $2e$ -periodic supercurrent is observed at zero bias along with  $e$ -periodic features at finite bias due to a combination of Josephson quasiparticle (JQP) resonances and Coulomb blockade of quasiparticle tunneling [Fig. 2(a)]. Similar behavior was seen in a number of other devices. The 4.2 K resistance of this device was 47 k $\Omega$  and the charging energy  $E_c = e^2/2C_\Sigma = 77$   $\mu$ eV, as determined from normal-state Coulomb diamonds measured at  $B = 2.5$  T. Estimating the Josephson energy per junction from the 4.2 K resistance and the Ambegoakar-Baratoff relation ( $E_J \sim \frac{\hbar\Delta_j\Delta_j}{4(\Delta_j+\Delta_j)e^2R}$ ) we find  $E_J = 33$   $\mu$ eV.

Taking a single trace over the supercurrent oscillations at  $V_{ds} = 0$  [Fig. 2(b)], a change in polarity of the mixer output occurs indicating a phase shift of the reflected rf carrier. Further investigation with a network analyzer

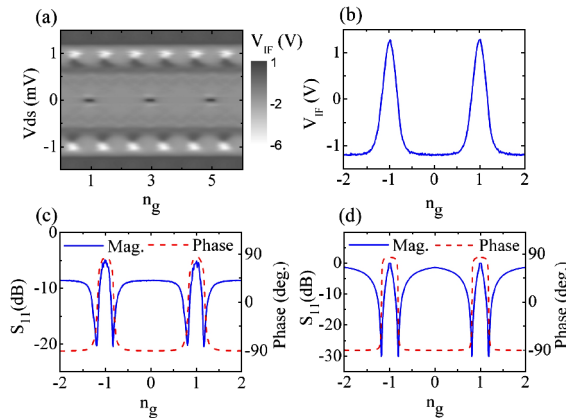


FIG. 2 (color online). (a) Coulomb diamonds showing the  $2e$ -periodic supercurrent at zero-bias and  $e$ -periodic transport at finite bias. (b) Amplified mixer output for  $V_{ds} = 0$  showing the form of the supercurrent oscillations. (c) Network analyzer measurement (heavily averaged) of magnitude and phase of rf carrier across the supercurrent oscillations. The incident power is  $-107$  dBm. (d) Model of the amplitude and phase response across the supercurrent oscillations.

[Fig. 2(c)] shows large changes in both the amplitude and phase across the supercurrent oscillations. For the amplitude component, there is a high reflection coefficient at both  $n_g = 1$  (on supercurrent maxima) and  $n_g = 0$ , and a minima in reflection coefficient on the sides of the supercurrent oscillation. There is also a large phase shift ( $\delta\theta = 178^\circ$ ) between  $n_g = 1$  and  $n_g = 0$ , with the phase shifts coinciding with the amplitude minima.

To understand the behavior of this circuit we develop a model in which the rf response depends on the ratio of the driving current ( $I_{rf} \sim V_{rf}/\omega L = 1$  nA at  $-107$  dBm) to the switching current ( $I_{sw}$ ) of the SCPT. We calculate switching currents using a 2-band model of the SCPT [7] finding a maximum  $I_{sw} \sim 5$  nA for the ground band at  $n_g = 1$ . If  $I_{rf} < I_{sw}$ , we assume the SCPT remains in current mode and presents zero resistance. This is impedance transformed by the tank circuit to yield  $Z_T \sim \infty$  and causes almost complete reflection.

In the case where  $I_{rf} > I_{sw}$ , we assume a hysteresis loop at the carrier frequency in which the device is partly [for  $I_{rf}(t) < I_{sw}$ ] in current mode and partly in voltage mode [for  $I_{rf}(t) > I_{sw}$ ]. This leads to an average resistance  $\langle R \rangle$  which is transformed by the tank circuit to  $Z_T = L/\langle R \rangle C$ . Using  $I_{sw}$  from the 2-band model, an expression for  $\langle R \rangle$  [18] and the tank circuit parameters, we simulate the amplitude and phase response of the device [Fig. 2(d)]. We note a reduced value of  $E_J = 8$   $\mu$ eV was taken to account for the suppression of  $I_{sw}$  due to environmental effects. The amplitude and phase response are well modeled, with the large phase shift occurring as the resonant circuit changes between under ( $n_g = 0, \langle R \rangle > 1$  M $\Omega$ ) and over damping ( $n_g = 1, \langle R \rangle = 0$   $\Omega$ ). A phase shift is expected in the SCPT due to the Josephson inductance [19];

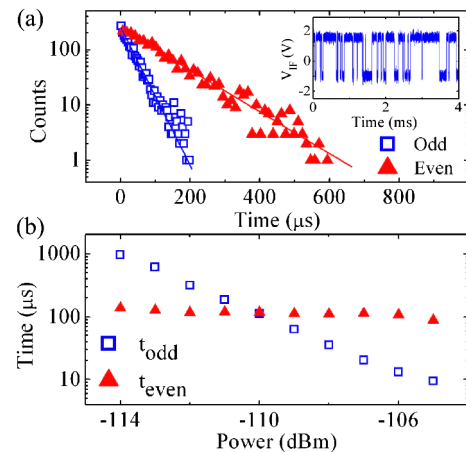


FIG. 3 (color online). (a) A histogram of times spent in both the even and odd states; the solid lines are fitted exponentials. Inset: switching between even and odd states observed in non-averaged measurements at  $n_g = 1$  with an incident rf carrier power of  $-108$  dBm. (b) The time constants, deduced from the previous histogram, as a function of the rf carrier power.

however, in this case it can be explained by the resonant circuit going through critical damping.

Charge sensitivity is determined by applying a 1 MHz gate signal of  $0.026e$  rms and measuring the signal to noise ratio (SNR) of the resulting sidebands with a spectrum analyzer. Since there is a phase component to our signal we perform this measurement after demodulation. Using the formula  $\Delta q_{\text{rms}} \times 10^{-\text{SNR}/20} / \sqrt{2B}$ , where  $B$  is resolution bandwidth, we find a sensitivity of  $1.5 \times 10^{-5} e \text{ Hz}^{-0.5}$  which is comparable to superconducting and normal-state rf-SETs [17].

Two-level switching behavior occurs with the device biased on a supercurrent peak and  $V_{\text{IF}}$  monitored as a function of time. The inset in Fig. 3(a) shows a representative 4 ms time record. The positive level at  $V_{\text{IF}} = 1.6$  V corresponds to the top of the supercurrent peak while the negative level  $V_{\text{IF}} = -1.0$  V corresponds to the signal in the trough between peaks. We attribute the positive voltage state to an even (unpoisoned) state where there are only Cooper pairs on the island. By contrast, negative voltages correspond to a ‘‘poisoned state’’ where a single quasiparticle occupies the island and the supercurrent peak is shifted from  $n_g = 1$  to  $n_g = 0$ . We record traces of length 400 ms, consisting of  $10^6$  data points, in order to obtain reliable statistics.

State parity is ascertained by comparing  $V_{\text{IF}}$  to a threshold halfway between the even and odd levels. The distribution of times spent in the even and odd states is measured and plotted in a histogram [Fig. 3(a)]. We fit an exponential decay  $e^{-t/t_i}$  to the histogram, using the parameter  $t_i$  to define the even and odd-state lifetimes. For the data in Fig. 3(a)  $t_{\text{odd}} = 35 \mu\text{s}$  and  $t_{\text{even}} = 110 \mu\text{s}$ . The data are well fitted indicating that the tunnel processes obey Poissonian statistics. A recent study of two-level systems has shown that finite receiver bandwidth can have a significant effect on time constants resulting from an analysis of this type [20]. The majority of time constants measured are  $>10 \mu\text{s}$  and our receiver bandwidth is 1 MHz hence, using the analysis in [20], we expect the resulting systematic error to be  $<10\%$ .

We measure the even- and odd-state lifetimes as a function of rf-carrier power to investigate the effect of the rf measurement [Fig. 3(b)]. A strong reduction in  $t_{\text{odd}}$  and only a slight reduction in  $t_{\text{even}}$  is noticed. The likely cause of reduction of the odd-state lifetime is that the rf carrier causes heating which thermally activates a quasiparticle off the island. The small reduction in  $t_{\text{even}}$  indicates that the rf carrier does not significantly increase the quasiparticle population in the leads, and any increase in temperature does not strongly affect the poisoning rate.

With the aim of determining the thermal activation of the poisoning and unpoisoning events we study the even- and odd-state lifetimes as a function of temperature. A low rf power ( $-112$  dBm) was chosen to minimize heating by the carrier signal. A reduction in  $t_{\text{odd}}$  occurs as the temperature is increased, which agrees with the measurements

in [12] and is due to thermal excitation of quasiparticles out of the quasiparticle trap formed on the island [Fig. 4(a)]. Considering the free energy change of this transition, we expect the time constant to be approximately  $t_{\text{odd}} = \frac{e^2 R}{2} \times \frac{\exp(\delta E/kT) - 1}{\delta E}$  [21], where  $\delta E$  is the quasiparticle trap depth, and  $R$  the average tunnel junction resistance. Fitting the data [22] to this thermal activation model we find an experimental value of  $\delta E = 50 \pm 4 \mu\text{eV}$  for the trap depth. The expected quasiparticle trap depth can be determined by considering the energy difference between the poisoned and unpoisoned states [11]. At the supercurrent peak ( $n_g = 1$ ) the maximum unpoisoned energy (corresponding to the excited state, and assuming no superconducting phase difference across the device) is  $E_u = E_c + \frac{E_J}{2}$ , while the poisoned-state energy has a minimum energy of  $E_p = \delta\Delta = \Delta_i - \Delta_l$ . It is useful to note that trap depth changes with gate bias ( $n_g$ ) and an investigation of this was carried out in [12]. For our analysis we use the values of  $E_c = 77 \mu\text{eV}$  and  $E_J = 33 \mu\text{eV}$  measured for the SCPT and  $\delta\Delta = 42 \pm 18 \mu\text{eV}$  as measured from the SIS junctions. Calculating  $\delta E = E_u - E_p$  a quasiparticle trap with depth  $52 \pm 18 \mu\text{eV}$  is expected, hence close agreement to the experimental value is shown.

A constant  $t_{\text{even}}$  is measured up to  $T \sim 180$  mK, with the value being reduced by thermal activation at higher temperatures. The poisoning rate is expected to depend linearly on both the tunnel barrier conductance  $G_i$  (taken to be in units of  $\frac{e^2}{h}$ ) and the density of quasiparticles in the leads. An expression for the poisoning rate was deduced in [6] to be  $t_{\text{even}}^{-1} \approx AT^{1/2} \exp(-\Delta_l/kT)$  for the case where temperature is small compared to trap depth ( $kT \ll E_u - E_p$ ) and  $A = \frac{G_1 + G_2}{4\hbar} \sqrt{\frac{k\Delta_l}{2\pi}} \sqrt{\frac{E_u - E_p}{\Delta_l + \Delta_i + E_u}}$ . The temperature

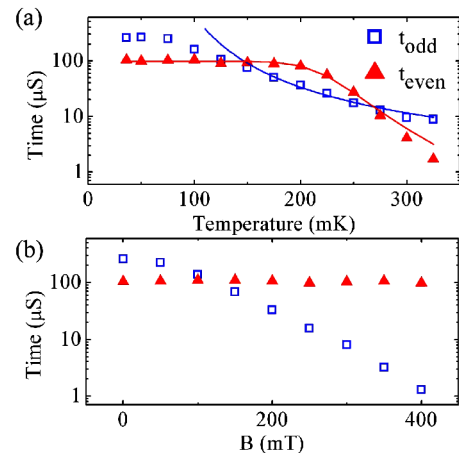


FIG. 4 (color online). (a) The time constants  $t_{\text{even}}$  and  $t_{\text{odd}}$  determined as a function of temperature with an rf-carrier power of  $-112$  dBm. The fit to  $t_{\text{odd}}$  is from a model of thermal activation of quasiparticles off the island. For  $t_{\text{even}}$ , the fitted line includes both a constant quasiparticle poisoning rate and thermal activation of quasiparticles across the superconducting gap. (b) Even and odd lifetimes as a function of magnetic field.

dependence of the poisoning rate can be explained by a constant low-temperature quasiparticle population (causing rate  $t_c^{-1}$ ) and, at higher temperatures, the presence of thermally excited quasiparticles. Adding the rates due to these two populations we obtain  $t_{\text{even}}^{-1} = t_c^{-1} + AT^{1/2} \exp(-\Delta_l/kT)$ . Figure 4(a) shows a fit to the data, with all parameters free, and shows good agreement with some deviation above 300 mK. The parameters we deduce from the fit are a constant low-temperature even-state lifetime of  $t_c = 102 \pm 2 \mu\text{s}$ ,  $A = 1.8 \pm 0.2 \times 10^{20} \text{ K}^{-0.5} \text{ s}^{-1}$ , and  $\Delta_l = 213 \pm 31 \mu\text{eV}$ . The value of  $\Delta_l$  is in close agreement with the measurements from the SIS junctions. The calculated value of  $A$  is  $0.92 \times 10^{20} \text{ K}^{-0.5} \text{ s}^{-1}$ , hence we see approximate agreement between the theory and the temperature dependent experimental poisoning rate. Poisoning rate (slightly) increases with trap depth in this regime and the theoretical underestimate may be related to the greater trap depth indicated by measurement of  $t_{\text{odd}}$ .

We are able to define an effective quasiparticle temperature ( $T_{qp}$ ). This is the temperature that causes a quasiparticle tunneling rate, due to the thermal excitation of quasiparticles in the leads, equal to the constant low-temperature value [ $t_c^{-1} = AT_{qp}^{1/2} \exp(-\Delta_l/kT_{qp})$ ]. For this device  $T_{qp} = 228 \text{ mK}$ , which is slightly greater than the electron temperature ( $T_e \sim 150 \text{ mK}$ ) as estimated from the fit to  $t_{\text{odd}}$ . Because of the relatively long recombination time of quasiparticles (1–10  $\mu\text{s}$ ) [23], quasiparticles created by microwave radiation in the leads can cause  $T_{qp} > T_e$ . For previous measurements (on devices with unengineered  $\Delta$ ) in which a lack of poisoning was observed, e.g., [7], either a low quasiparticle temperature was achieved or measurement bandwidth was insufficient to resolve poisoning events.

We also perform a quantitative study of the even- and odd-state lifetimes in the presence of an in-plane magnetic field, noting that magnetic fields have previously been used to change the periodicity of CPBs [14]. Little change is noticed in  $t_{\text{even}}$  as the field is increased [Fig. 4(b)]. Presumably the poisoning rate remains approximately constant until the quasiparticle trap becomes a barrier and quasiparticles have to be thermally excited onto the island. However, there is a large reduction of  $t_{\text{odd}}$ , indicating that the quasiparticle trap becomes shallower and quasiparticles can more easily be thermally excited out. For thinner films the critical field increases [13], indicating a greater reduction in  $\Delta_l$  than  $\Delta_i$  (effectively increasing  $\delta\Delta$ ) at finite fields. For example, performing a fit to a temperature dependence of  $t_{\text{odd}}$  at  $B = 150 \text{ mT}$ , we find a reduced value of  $\delta E = 27 \pm 2 \mu\text{eV}$ .

In summary, we employed the change in  $\Delta$  with aluminum film thickness to fabricate a SCPT with a reduced quasiparticle trap on the island. Individual quasiparticle poisoning events were measured and the resulting statistics analyzed to determine time constants for the even- and odd-state lifetimes. An important aspect of the experiment was measurement of the thermal activation of poisoning

rate. This enabled a quasiparticle temperature to be determined which will be a useful parameter to compare different devices and experimental setups. Furthermore, we expect that by reducing the island film thickness (increasing  $\delta\Delta$ ) to create a quasiparticle barrier on the island, or by introducing quasiparticle traps (therefore increasing  $t_{\text{even}}$ ), we will be able to fabricate SCPTs and CPBs with negligible quasiparticle poisoning.

The authors would like to thank A. C. Doherty, G. J. Milburn, O. Naaman, J. Aumentado, R. Lutchyn, and D. Reilly for helpful discussions and D. Barber and R. P. Starrett for technical support. This work is supported by the Australian Research Council, the Australian Government, and by the US National Security Agency (NSA) and US Army Research Office (ARO) under Contract No. DAAD19-01-1-0653.

---

\*Electronic address: andrew.ferguson@unsw.edu.au

- [1] Y. Nakamura, Y.A. Pashkin, and J.S. Tsai, *Nature* (London) **398**, 786 (1999).
- [2] A. Wallraff *et al.*, *Nature* (London) **431**, 162 (2004).
- [3] A. B. Zorin, *Phys. Rev. Lett.* **86**, 3388 (2001).
- [4] J. Mannik and J. E. Lukens, *Phys. Rev. Lett.* **92**, 057004 (2004).
- [5] R. Lutchyn, L. Glazman, and A. I. Larkin, *Phys. Rev. B* **74**, 064515 (2006).
- [6] R. Lutchyn, L. Glazman, and A. Larkin, *Phys. Rev. B* **72**, 014517 (2005).
- [7] P. Joyez *et al.*, *Phys. Rev. Lett.* **72**, 2458 (1994).
- [8] T. M. Eiles and J. M. Martinis, *Phys. Rev. B* **50**, 627 (1994).
- [9] A. Amar *et al.*, *Phys. Rev. Lett.* **72**, 3234 (1994).
- [10] M. Tuominen *et al.*, *Phys. Rev. Lett.* **69**, 1997 (1992).
- [11] J. Aumentado *et al.*, *Phys. Rev. Lett.* **92**, 066802 (2004).
- [12] O. Naaman and J. Aumentado, *Phys. Rev. B* **73**, 172504 (2006).
- [13] R. Meservey and P. M. Tedrow, *J. Appl. Phys.* **42**, 51 (1971).
- [14] D. Gunnarsson *et al.*, *Phys. Rev. B* **70**, 224523 (2004).
- [15] A. J. Ferguson *et al.*, *Phys. Rev. Lett.* **97**, 086602 (2006).
- [16] R. J. Schoelkopf *et al.*, *Science* **280**, 1238 (1998).
- [17] L. Roschier *et al.*, *J. Appl. Phys.* **95**, 1274 (2004).
- [18] For the hysteresis loop described, and assuming a retrapping of the current mode at  $V_{ds} = 0$ ,  $\langle R \rangle^2 \approx (\omega L)^2 \times (\sin^{-1} \frac{I_{sw}}{I_{rf}} - \frac{I_{sw}}{I_{rf}} \sqrt{1 - \frac{I_{sw}}{I_{rf}}})^{-1}$ .
- [19] M. A. Sillanpaa, L. Roschier, and P. J. Hakonen, *Phys. Rev. Lett.* **93**, 066805 (2004).
- [20] O. Naaman and J. Aumentado, *Phys. Rev. Lett.* **96**, 100201 (2006).
- [21] H. Grabert and M. H. Devoret, *Single Charge Tunneling* (Plenum, New York, 1992), pp. 1–18.
- [22] Assuming saturation of the electron temperature and heating effects associated with the rf carrier we only fit the higher temperature data points ( $T \geq 150 \text{ mK}$ ).
- [23] J. L. Levine and S. Y. Hsieh, *Phys. Rev. Lett.* **20**, 994 (1968).